

## The Jodrell Bank – IAC 33 GHz Interferometer

D. L. Harrison<sup>1</sup>, R. A. Watson<sup>1</sup>, J. A. Rubiño-Martin<sup>2</sup>, J. F. Macias-Perez<sup>1</sup>, R. D. Davies<sup>1</sup>, R. Rebolo<sup>2</sup>, C. M. Gutiérrez<sup>2</sup>, R. J. Davis<sup>1</sup>

<sup>1</sup> *Jodrell Bank Observatory, Manchester University, Macclesfield, UK*

<sup>2</sup> *Instituto de Astrofísica de Canarias, 38200 La Laguna, Tenerife, Canary Islands, Spain*

**Abstract.** This paper presents results obtained with the Jodrell Bank – IAC two-element 33 GHz interferometer, located at the Teide Observatory on Tenerife, which is designed to measure the level of the Cosmic Microwave Background (CMB) fluctuations on angular scales of 1° and 2°. The result from a maximum likelihood analysis of observations taken at Dec +41° of  $\Delta T_\ell = 63_{-6}^{+7} \mu\text{K}$  at  $\ell = 208 \pm 18$  is comparable with those of Boomerang and Maxima. The contribution of possible foreground contaminants are considered.

### 1. A Description of the Interferometer

The interferometer consists of two horn-reflector antennas positioned to form a single E–W baseline, which has two possible lengths depending on the separation of the horns. The narrow spacing configuration has a baseline of 152 mm, 16.5 wavelengths, while in the wide spacing configuration the horns are 304 mm, 32.9 wavelengths, apart. Observations are made at a fixed declination using the rotation of the Earth to “scan” 24 hours in RA each day. The horn polarization is horizontal – parallel with the scan direction. There are two data outputs representing the cosine and the sine components of the complex interferometer visibility. The operating frequency range is 31–34 GHz, near a local minimum in the atmospheric emission spectrum. The low level of precipitable water vapour, which is typically around 3 mm at Teide Observatory permits the collection of high quality data, limited by the receiver noise for more than 80 per cent of the time.

The measured response of the interferometer is well approximated by a Gaussian with sigmas of  $\sigma_E = 2^{\circ}25 \pm 0^{\circ}03$  (in RA) and  $\sigma_H = 1^{\circ}00 \pm 0^{\circ}02$  (in Dec), modulated by fringes with a period of  $f = 3^{\circ}48 \pm 0^{\circ}04$  in RA at a baseline of 152 mm and  $f = 1^{\circ}74 \pm 0^{\circ}02$  in RA at a baseline of 304 mm. This defines the range of sensitivity to the different multipoles  $\ell$  of the CMB power spectrum ( $C_\ell$ ) of the narrow and wide spacings to a maximum sensitivity at  $\ell = 106$  (1°6) and half sensitivity at  $\Delta\ell = \pm 19$ , and at  $\ell = 208$  (0°8)  $\pm 18$ , respectively.

A known calibration signal (CAL) is periodically injected into the waveguide after the horns allowing a continuous calibration and concomitant corrections for drifts in the system gain and phase offset. A full description of the instrument configuration can be found in Melhuish et al. (1999).

## 2. Basic Data Processing & Calibration

The first step in the analysis is the removal of any variable baseline offsets from the data and the correction of a small departure from quadrature between the cosine and sine data. The data are calibrated relative to the CAL signal and rebinned into 2-minute bins to ensure alignment in RA between successive scans. The effects of the Sun and bad weather are removed and individual scans are averaged to form a “stack”. The CAL signal itself needs to be calibrated by an astronomical source. The small collecting area of the antenna gives a reduced sensitivity to point sources and many days of observation are required to achieve a signal-to-noise ratio sufficient for calibration purposes. Consequently, the Moon is used as the primary calibrator as the power received from a single Moon transit is large enough to give signal-to-noise ratios of  $\sim 6000 : 1$ . The model used for the Moon brightness temperature at 33 GHz is that of Gorenstein & Smoot (1981). Regular observations of the Moon were made; using 27 observations of the Moon, an average amplitude for CAL of  $14.7 \pm 0.8$  K was found. A more complete discussion of the basic data processing and calibration can be found in Dicker et al. (1999) and Harrison et al. (2000).

## 3. The effect of foregrounds on the data

The sensitivity of the interferometer to foreground contaminants, depends of the baseline used. The wide spacing is less sensitive than the narrow spacing to Galactic diffuse emission such as dust, free-free and synchrotron, but is more sensitive to the contribution from point sources.

The 6 strongest sources with  $S(33 \text{ GHz}) \geq 2$  Jy within a  $6^\circ$  strip centred on Dec  $+41^\circ$  are routinely monitored by the Metsahovi programme at 22.0 and 37.0 GHz. Using these data over the period of our observations, it was possible to assess their flux densities at 33 GHz. These were then convolved with the two-dimensional interferometer beam pattern and converted to antenna temperatures; in this form these sources may be subtracted from the data. The contribution of weaker point sources was estimated according to the results of Franceschini et al. (1989). At 33 GHz and at resolutions of  $0.8$  and  $1.6$  these are expected to be  $\Delta T \sim 11 \mu\text{K}$  and  $\Delta T \sim 8 \mu\text{K}$  respectively. These contributions add in quadrature to the CMB signal, giving a contribution from unresolved sources of  $1 \mu\text{K}$  at  $\ell \sim 200$  and  $0.5 \mu\text{K}$  at  $\ell \sim 100$ .

An estimate of the amplitude of the diffuse Galactic component in our data can be computed using the results obtained in the same region of the sky by the Tenerife CMB experiments (Gutiérrez et al. 2000). At 10.4 GHz and on angular scales centred on  $\ell = 20$  the maximum Galactic component was estimated to be  $\leq 28 \mu\text{K}$ . Assuming that this contribution is entirely due to free-free emission ( $\beta = -2.1$ ) and a conservative Galactic spatial power spectrum of  $\ell^{-2.5}$ , the predicted maximum Galactic contamination in the data is  $0.8 \mu\text{K}$  at  $\ell \sim 200$  and  $2 \mu\text{K}$  at  $\ell \sim 100$ . Any such contribution would add in quadrature to that from the CMB, and so is insignificant. The true make-up of the 10.4 - GHz Galactic foreground emission will have a steeper average spectral index since synchrotron radiation with  $\beta \sim -3$  will contribute to the measured value, therefore the contribution to our result will be even lower than stated. The

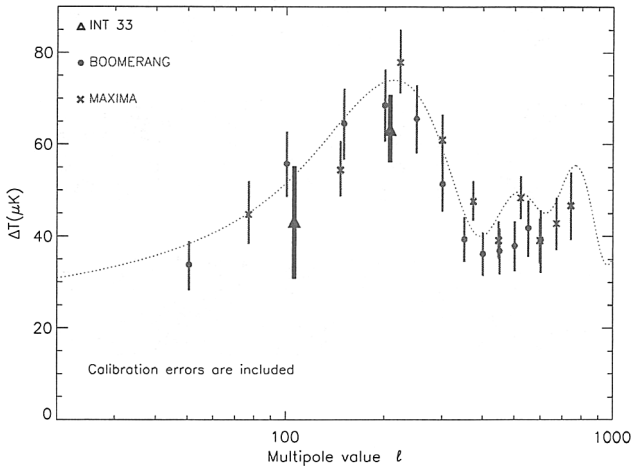


Figure 1. Our results at  $\ell = 106$  and  $\ell = 208$  as published in Dicker et al. (1999) and Harrison et al. (2000) compared with the recently published results from the Boomerang (de Bernardis et al. 2000) and the Maxima (Hanany et al. 2000) experiments; calibration errors have been included. The dotted line represents the model given by  $\Omega_b = 0.05$ ,  $\Omega_{\text{CDM}} = 0.40$ ,  $\Omega_\lambda = 0.55$  and  $H_0 = 70 \text{ km s}^{-1} \text{ Mpc}^{-1}$ ; this is shown for illustrative purposes and does not represent a fit to the data.

Table 1. Values of  $\Delta T$  from Boomerang and Maxima, including calibration errors, compared with the results from the interferometer.

Experiment	Calibration uncertainty	$\Delta T$ around $\ell \sim 200$ ( $\mu\text{K}$ )	$\ell$
Int33	6%	$63^{+8}_{-7}$	208
Boomerang	10%	$69^{+8}_{-8}$	200
MAXIMA	4%	$78^{+7}_{-7}$	223

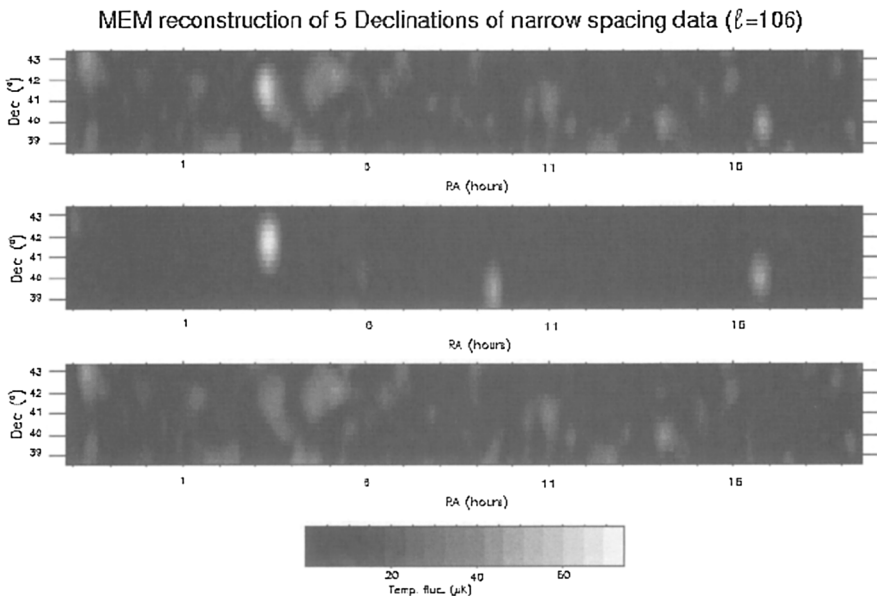


Figure 2. The top plot shows a MEM reconstruction of 5 declinations of narrow spacing data from Dec  $+38^{\circ}6$  to  $+43^{\circ}4$ . The expected contribution from the 6 strongest point sources are shown in the centre plot and the MEM reconstruction of the point source subtracted data is shown below.

interferometer has observed Dec  $+41^{\circ}$  with both the wide and narrow spacing configurations. These data are analysed in Harrison et al. (2000) and Dicker et al. (1999) using a maximum likelihood approach. The results of which, after the contribution from point sources has been excluded, are shown in Figure 1 compared with the recently published results from the Boomerang (de Bernardis et al. 2000) and Maxima (Hanany et al. 2000) experiments. Table 1 shows the values of  $\Delta T$ , including calibration errors, around  $\ell \sim 200$ ; our result of  $\Delta T = 63.0^{+8.0}_{-7.0} \mu\text{K}$  at  $\ell = 208 \pm 18$  is comparable with that of Boomerang, which found an amplitude for the first peak of  $\Delta T = 69 \pm 8 \mu\text{K}$  at  $\ell = 197 \pm 6$  and Maxima, which found a peak at  $\ell \approx 220$  of amplitude  $\Delta T = 78 \pm 7 \mu\text{K}$ .

The interferometer has observed 4 declinations adjacent to Dec  $+41^{\circ}$  at  $2^{\circ}$  resolution. A maximum entropy (MEM) reconstruction of these 5 declinations from  $+38^{\circ}6$  to  $+43^{\circ}4$  is shown in Figure 2. The central plot in Figure 2 shows the point sources as observed by the Metsahovi monitoring programme as discussed above convolved with the two-dimensional interferometer beam pattern. The lower plot shows the MEM reconstruction of the point source subtracted data. These data will be the subject of a forthcoming paper and should reduce the sample variance in the  $\ell \sim 100$  (Dicker et al. 1999) result to  $\sim 5\%$ .

**Acknowledgments.** This work has been supported by the European Community Science program contract SCI-ST920830, the Human Capital and Mobility contract CHRXCT920079 and PPARC. We thank Dr. H. Teräsraanta for providing data on point sources at 22 and 37 GHz.

## References

- de Bernardis, P. et al., 2000, *Nature*, 404, 955  
Dicker, S. R. et al., 1999, *MNRAS*, 309, 750  
Franceschini, A., Toffolatti, L., Danese L. & De Zotti, G. 1989, *ApJ*, 344, 35  
Gorenstein, M. V. & Smoot G. F. 1981, *ApJ*, 244, 361  
Hanany, S. et al., 2000, *astro-ph / 0005123*  
Harrison, D. L. et al. 2000, *MNRAS*, 316, L24  
Melhuish, S. J. et al. 1999, *MNRAS*, 305, 399